

Coupled models of heat transfer and phase transformation for the run-out table in hot rolling^{*}

Shui-xuan CHEN, Jun ZOU^{†‡}, Xin FU

(State Key Laboratory of Fluid Power Transmission and Control, Zhejiang University, Hangzhou 310027, China)

[†]E-mail: junzou@zju.edu.cn

Received Oct. 30, 2007; revision accepted Jan. 18, 2008

Abstract: Mathematical models are been proposed to simulate the thermal and metallurgical behaviors of the strip occurring on the run-out table (ROT) in a hot strip mill. A variational method is utilized for the discretization of the governing transient conduction-convection equation, with heat transfer coefficients adaptively determined by the actual mill data. To consider the thermal effect of phase transformation during cooling, a constitutive equation for describing austenite decomposition kinetics of steel in air and water cooling zones is coupled with the heat transfer model. As the basic required inputs in the numerical simulations, thermal material properties are experimentally measured for three carbon steels and the least squares method is used to statistically derive regression models for the properties, including specific heat and thermal conductivity. The numerical simulation and experimental results show that the setup accuracy of the temperature prediction system of ROT is effectively improved.

Key words: Run-out table (ROT), Cooling process, Heat transfer, Phase change, Material properties

doi:10.1631/jzus.A0720046

Document code: A

CLC number: TH137

INTRODUCTION

In the process of continuous hot slab rolling, temperature is one of the most important parameters controlling the kinetics of metallurgical transformations and the flow stress of the rolled metal (Sun *et al.*, 2002; Chen *et al.*, 2006). The run-out table (ROT) acts as an effective metallurgical tool to control the desired temperature of the cooled strip so as to obtain the appropriate transformation product due to phase change (Mukhopadhyay and Sikdar, 2005).

To obtain an adequate performance of the temperature control system on ROT, it is vital to develop physical models capable of reproducing heat transfer and metallurgical phenomena (Serajzadeh, 2003). Modeling for the precise prediction of such behavior, however, is a difficult task, due to nonlinear heat transfer problems involving variation of thermal ma-

terial properties and phase transformation from austenite to lower temperature phases, i.e., ferrite, pearlite or bainite during the cooling process (Moaveni, 2005). The conventional temperature model used in a hot mill is in algebraic or exponential form, assuming a uniform distribution along the strip thickness and neglecting the phase changes during the cooling process. Besides, temperature-dependent properties data are rare and, when available, they are often provided only for room temperature. This compromises remarkably the accuracy and relevance of theoretical predictions (Tan *et al.*, 2005).

The present work is aimed at building mathematical models with high accuracy, taking into account the heat transfer and phase evolution behavior in both thickness and width of a strip on ROT in a hot strip mill. The variational calculus and the finite element method have been employed to solve the governing heat transfer equation. Meanwhile, the austenite phase transformation of steel in air and water cooling zones is coupled with the heat transfer model. Then an iterative procedure is adopted to deal

[†] Corresponding author

^{*} Project supported by the National Basic Research Program (973) of China (No. 2006CB705400) and the National Natural Science Foundation of China (No. 50575200)

with the temperature-dependent material properties during cooling as well as with the coupled temperature-transformation relationship. The FORTRAN codes are developed to obtain the numerical solution. Furthermore, experiments are performed to determine thermal material properties such as specific heat, thermal conductivity and density of the metal being rolled for three industrial carbon steels. Finally, the log data was obtained from a 2050 mm hot strip mill at Baoshan Iron & Steel Co. Ltd. (Bao Steel) and the measured coiling temperature was compared with that calculated by the models.

COOLING SYSTEM DESCRIPTION

The general arrangement of the cooling system of an ROT in a specific metallurgical industry is simplified in Fig.1. The cooling section consists of 19 cooling zones with different cooling effects. The first 16 zones equipped with 136 valves are employed as the main cooling system and the last 3 zones with 24 valves are employed as finish cooling. The last 3 zones with 24 valves are used to reduce the strip temperature to close to the desired coiling temperature. The water flow rate for the top and bottom valves is about 7000 m³/h. The cooling-water pressure is 7×10⁴ Pa.

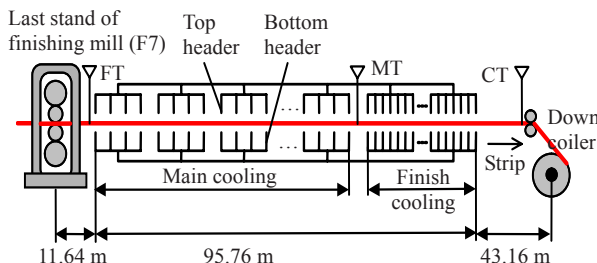


Fig.1 Schematic diagram of the ROT

The first cooling bank is located at a distance of 11.64 m from the last finishing stand (F7). The total cooling section is 95.76 m and the distance between the last cooling header and the down coiler is 43.16 m. To ascertain the strip temperature along the ROT, pyrometers are placed at the beginning to measure finishing temperature (FT), at the end to measure coiling temperature (CT), and at some intermediate positions to measure middle temperature (MT), although temperature measurement at these points is difficult and imprecise due to the radiation effect of the steam over the strip (Prieto *et al.*, 2001).

MATHEMATICAL MODEL DEVELOPMENT

Heat transfer formulation

The general form of energy equation for 2D transient heat transfer in a cooled strip with thermal material properties dependent on temperature is given as (Singh *et al.*, 2006)

$$D[T(x,y,t)] = \lambda \left(\frac{\partial^2 T}{\partial x^2} + \frac{\partial^2 T}{\partial y^2} \right) + \dot{q}_t - \rho c \frac{\partial T}{\partial t} = 0, \quad (1)$$

where T is the temperature, K; x and y are the coordinates of thickness and width directions, respectively; t is the time, s; λ is the thermal conductivity, W/(m·K); c is the specific heat, J/(kg·K); ρ is the density of the rolled metal, kg/m³; \dot{q}_t is the rate of heat of transformation, kJ/kg. In Eq.(1), the heat generation term \dot{q}_t is an important heat source on ROT accounting for the heat generated due to the phase transformation from austenite to ferrite, pearlite or bainite during cooling.

To solve this partial differential equation, it is vital to know the initial and boundary conditions. The initial condition is the temperature distribution along the thickness direction after the last finishing stand, i.e., $T(x,y=0, t=0)=T_0(x)$. The boundary conditions are the air radiation and water convection heat transfer equations, which can be expressed as Eqs.(2) and (3), respectively

$$-\lambda \frac{\partial T}{\partial x} = h_\infty (T - T_\infty) + \sigma \varepsilon (T^4 - T_\infty^4), \quad (2)$$

$$\begin{cases} -\lambda \frac{\partial T}{\partial x} = h_{w1} (T - T_{w1}), \\ -\lambda \frac{\partial T}{\partial x} = h_{w2} (T - T_{w2}), \end{cases} \quad (3)$$

where T_∞ is the surrounding temperature, K; T_{w1} , T_{w2} are water temperatures in the impingement zone and in the stable film zone, respectively, K; ε and σ are the emissivity factor and the Stefan-Boltzmann constant, respectively; h_∞ is the surrounding heat transfer coefficient, W/(m²·K); h_{w1} and h_{w2} are convection heat transfer coefficients in the impingement zone and in the stable film zone, respectively, W/(m²·K).

The weak form of Eq.(1) can be written as:

$$\int_{\Omega} W_t \left[\lambda \left(\frac{\partial^2 T}{\partial x^2} + \frac{\partial^2 T}{\partial y^2} \right) + \dot{q}_t - \rho c \frac{\partial T}{\partial t} \right] d\Omega = 0, \quad (4)$$

where W_t is the weight function; Ω is the 2D domain.

It should be noted that thermal conductivity and specific heat are experimentally tested in this study to be temperature-dependent properties. However, for each element these parameters can be assumed to be constants. The calculus of variations provides an alternative method for formulating the governing Eq.(1) and its boundary conditions. Variational calculus states that the minimization of the functional I can be obtained as

$$I = \int_{\Omega} \left[\frac{\lambda}{2} \left(\frac{\partial T}{\partial x} \right)^2 + \frac{\lambda}{2} \left(\frac{\partial T}{\partial y} \right)^2 - \dot{q}_t T + \rho c \frac{\partial T}{\partial t} T \right] d\Omega + \frac{1}{2} \int_{\Gamma} h(T - T_{\infty})^2 d\Gamma, \quad (5)$$

where Γ is boundary of the domain; h is the heat transfer coefficient.

The transversal profile of the cooled strip is discretized into E elements linked through m nodes. The element equation for the temperature distribution can be represented in vectorial form by $T^e = N^e T_i + N^e_j T_j = \mathbf{N}^e \mathbf{T}$, where T_i and T_j are the nodal temperatures to be determined and N the shape function matrix defined as $N = [N_1, N_2, N_3, \dots, N_m]$.

Eq.(5) must be minimized with respect to the set of nodal values \mathbf{T}

$$\frac{\partial I}{\partial \mathbf{T}} = \frac{\partial}{\partial \mathbf{T}} \sum_{e=1}^E I^e = \sum_{e=1}^E \frac{\partial I^e}{\partial \mathbf{T}} = 0, \quad (6)$$

The minimization process of Eq.(5) produces the following system of equations

$$\mathbf{M}\mathbf{T} + \mathbf{C} \frac{\partial \dot{\mathbf{T}}}{\partial t} = \mathbf{P}, \quad (7)$$

where \mathbf{M} is the conductance matrix, \mathbf{C} is the capacitance matrix and \mathbf{P} is the thermal load vector. The element contributions to \mathbf{M} , \mathbf{C} and \mathbf{P} are defined as

$$M^e = \int_{\Omega^e} \lambda \left(\frac{\partial N_i}{\partial x} \frac{\partial N_j}{\partial x} + \frac{\partial N_i}{\partial y} \frac{\partial N_j}{\partial y} \right) d\Omega$$

$$+ h \int_{\Gamma^e} N_i N_j d\Gamma, \quad (8)$$

$$C^e = \int_{\Omega^e} \rho c N_i N_j d\Omega, \quad (9)$$

$$P_i^e = \int_{\Omega^e} \dot{q}_t N_i d\Omega + h T_{\infty} \int_{\Gamma^e} N_i d\Gamma. \quad (10)$$

To discretize Eq.(7), Euler's method (Moaveni, 2005) for time integration of temperature is used

$$T^{p+1} = T^p + (1-\theta) \Delta t \dot{T}^p + \theta \Delta t \dot{T}^{p+1}, \quad (11)$$

where T^p is the temperature to be computed at time step p , θ is the Euler parameter and Δt is the time increment. The time discretized energy equation is then as follows

$$\left(\frac{1}{\theta \Delta t} \mathbf{C} + \mathbf{M} \right) T^{p+1} = \mathbf{C} \left(\frac{1}{\theta \Delta t} T^p + \frac{1-\theta}{\theta} \dot{T}^p \right) + \mathbf{P}. \quad (12)$$

The heat transfer model for the strip on ROT comprises air and water convections, internal conduction and external conduction with table rollers. During the cooling process the strip is firstly cooled, essentially by radiation, then the utilization of water leads to cooling by convection and radiation (top cooling and bottom cooling), and finally the predominant heat transfer mechanism is radiation. Previous research has confirmed that water cooling accounts for over 90% of the entire heat transfer (Mukhopadhyay and Sikdar, 2005).

After the exit from the last finishing stand, the strip travels a distance of 11.64 m (Fig.1) before it encounters the first laminar water jet, where water impinges on the strip and then separates into two streams which flow along the strip surface, as illustrated in Fig.2. v_f and w_f denote the average impinging speed and flow rate of cooling water, respectively. v_s denotes the travelling speed of the strip. The stagnation point is the point on the surface of the strip submerged in laminar water where the water velocity is zero. Due to the difference between the surface strip temperature and the saturation water temperature, the impingement of laminar water on the strip gives rise to boiling heat transfer characterized by three kinds of cooling zones (Mukhopadhyay and Sikdar, 2005):

(1) Impinging water jet zone (Zone 1): the highest heat fluxes area, where heat fluxes can

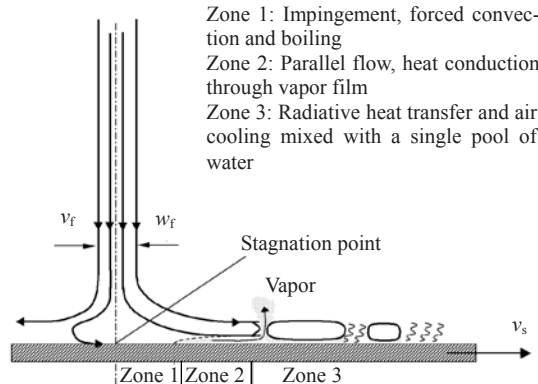


Fig.2 Heat transfer in water cooling area

achieve 20 MW/m².

(2) Parallel flow zone (Zone 2): heat conducts through vapour film and heat transfer rate reduces significantly; the typical values of heat fluxes are 200~600 kW/m².

(3) Air and water mixing zone (Zone 3): the water layer breaks up and the strip surface being exposed to air; heat transfer rates are about 10~50 kW/m².

The heat transfer coefficients in different cooling zones are functions of strip speed, surface temperature, water pressure and water temperature. However, it is difficult to account for the heat transfer coefficients analytically. An adaptive approach in multiplicative form has been made according to the specific cooling process of 2050 mm hot strip mill of Baosteel:

$$\alpha = \alpha_0 k_v k_T k_w k, \quad (13)$$

where α_0 is the heat transfer coefficient in an idealized set of conditions, k_v the correction for strip velocity, k_T the correction for the effect of water temperature, k_w the correction for the effect of a different valve type and water flow, k the general adaptive factor of the on-line adaptation model.

Phase transformation model

During the cooling process on ROT, the transformation of austenite into ferrite and pearlite exerts a significant influence on the thermal behavior of the cooling steel (Zhang et al., 2006). The internal heat source due to the phase transformation can be written as

$$\dot{q}_t = \Delta H_i \frac{dX_i}{dt}, \quad (14)$$

where ΔH_i is the amount of latent heat of transformation at a given temperature T_i , X_i is the transformed volume fraction expressed as a function of time.

The decomposition of austenite taking place in air cooling zones on ROT is approximated as isothermal transformation. The isothermal kinetics can be characterized by the Avrami equation (Han et al., 2002):

$$\frac{X}{X^e} = 1 - \exp(-kt^n), \quad (15)$$

where X is the transformed fraction and X^e the thermodynamic equilibrium fraction which can be determined from the equilibrium phase diagram at a given temperature and chemical composition. t is the elapsed time from the beginning of the transformation, k and n are material parameters that can be obtained for cooling steels on ROT from the time temperature transformation (TTT) diagram.

The decomposition of austenite taking place in water cooling zones is described as non-isothermal transformation behavior. Based on the theory advanced by Scheil, the non-isothermal transformation kinetics can be described as the sum of a series of small isothermal steps, on the assumption that the phase transformation is the isothermal kinetic reaction (Han et al., 2002). The transformed phase fraction up to the i th step, X_i , is expressed as follows:

$$\frac{X}{X^e} = 1 - \exp\left[-k_i\left(t'_i + \Delta t_i\right)^{n_i}\right], \quad (16)$$

$$t'_i = \left[-\frac{1}{k_i} \ln\left(\frac{1-X_{i-1}}{X_i^e}\right)\right]^{1/n}, \quad (17)$$

where t' is the equivalent transformation time needed to transform into the fraction of X_{i-1} at the temperature of the i th step, and Δt is the time step corresponding to the i th step.

Regarding the heat transfer equation, the temperature distribution within the cooling strip is affected by the discharged heat of the transformation (Serajzadeh, 2006). Furthermore, the amount of

transformation is a strong function of temperature. To solve the nonlinearly coupled problem, an iterative procedure in Fig.3 is adopted to deal with the temperature-dependent material properties during cooling as well as with the temperature-transformation relationship. Calculation continues until the temperature distribution in each time step converges to a constant condition.

MATERIAL AND EXPERIMENTS

It should be noted that the coupled mathematical models proposed in this paper rely heavily on thermo-physical parameters such as the specific heat, conductivity and density of the metal being rolled. These properties are often simplified as constants,

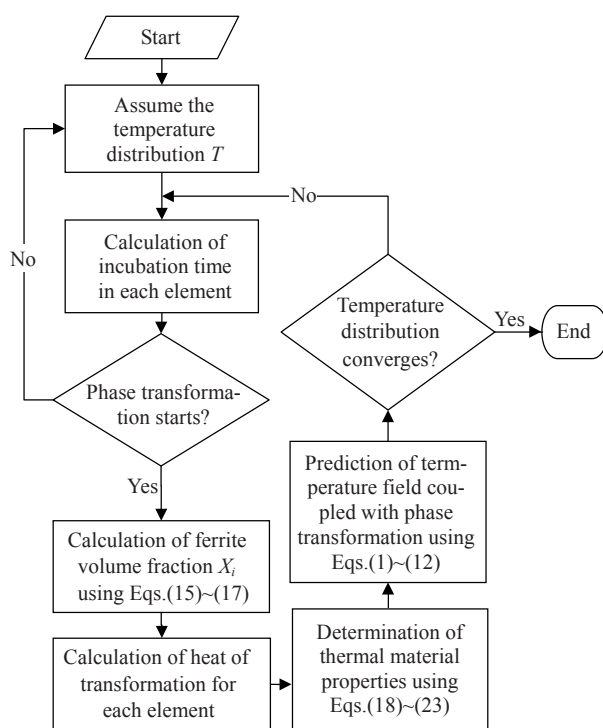


Fig.3 Iterative procedure for solving heat transfer and phase transformation

neglecting the influence of temperature. As a result, the accuracy of thermal models is remarkably reduced. Thus, in order to predict an accurate temperature history as well as the phase transformation kinetics, experiments have been done to provide accurate values of the physical properties of steels over the temperature range 0 °C~1000 °C.

Three example carbon steels produced in the 2050 mm hot strip mill of Bao Steel are chosen for experiments and analyses. Chemical composition of these tested steels is given in Table 1. Experiments are performed on the electro-thermo-mechanical test system and the least squares method has been used to statistically model the properties as functions of temperature.

For the working temperature range of the steel on ROT, the steel density hardly varies with temperature. Hence this property is approximated so as to be constant and only connected with the chemical composition of steels. The measured densities of three tested steels are 7879, 7865 and 7938 kg/m³, respectively.

Fig.4 shows thermal conductivity λ as function of temperature T for the three tested steels. It can be seen that the thermal conductivity decreases linearly with increasing temperature up to the turning point near 790 °C. Beyond that point the thermal conductivity increases slightly with temperature, again in a linear fashion but with a positive gradient. Empirical models of thermal conductivity are derived as follows:

Low carbon steel (0.047 wt% C):

$$\begin{cases} \lambda = -0.0325T + 51.875, & T \in [0, 790], \\ \lambda = -0.0026T + 26.061, & T \in [790, 1000]; \end{cases} \quad (18)$$

Medium carbon steel (0.220 wt% C):

$$\begin{cases} \lambda = -0.0335T + 50.4726, & T \in [0, 790], \\ \lambda = 0.0058T + 17.521, & T \in [790, 1000]; \end{cases} \quad (19)$$

High carbon steel (0.700 wt% C):

Table 1 Chemical composition of three carbon steels produced in the 2050 mm hot strip mill of Bao Steel

Carbon steel	Chemical composition (wt%)												
	C	Si	Mn	P	S	Al	Cr	Ni	Mo	V	Nb	Ti	N
Low	0.047	0.008	0.250	0.025	0.010	0.034	—	—	<0.005	<0.005	<0.002	<0.001	0.0033
Medium	0.220	0.075	0.730	0.015	0.008	0.029	0.019	0.013	0.004	—	—	0.011	0.0026
High	0.700	0.240	1.040	0.011	0.001	0.033	0.210	0.023	—	0.002	—	—	0.0023

$$\begin{cases} \lambda = -0.0253T + 42.9905, & T \in [0, 790], \\ \lambda = 0.0120T + 11.102, & T \in [790, 1000]. \end{cases} \quad (20)$$

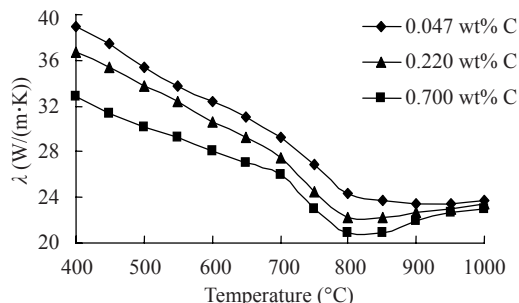


Fig.4 Steel conductivity as function of temperature

Fig.5 shows specific heat c as function of temperature T for the three tested steels. The specific heat also varies greatly with temperature and there is a change in the slope of the curves from 700 °C to 800 °C where phase transformation from austenite to ferrite takes place. Empirical models of specific heat are

Low carbon steel (0.047 wt% C):

$$\begin{cases} c = 0.9426T + 217.04, & T \in [0, 800], \\ c = -0.0865T^2 + 125.51T - 44461, & T \in [700, 800], \\ c = -0.0026T + 26.061, & T \in (800, 1000]; \end{cases} \quad (21)$$

Medium carbon steel (0.220 wt% C):

$$\begin{cases} c = 0.8613T + 254.8, & T \in [0, 800], \\ c = -0.1667T^2 + 242.05T - 87112, & T \in [700, 800], \\ c = 647.56, & T \in (800, 1000]; \end{cases} \quad (22)$$

High carbon steel (0.700 wt% C):

$$\begin{cases} c = 0.5168T + 416.37, & T \in [0, 800], \\ c = -0.4413T^2 + 638.25T - 228996, & T \in [700, 800], \\ c = 0.1675T + 470.32, & T \in (800, 1000]. \end{cases} \quad (23)$$

The above regression models are in good agreement with the measured data. Taking Eq.(21) as an example, the coefficients of determination (R^2) are 0.99921, 0.9933 and 0.9725, respectively. This indicates that the empirical models can predict approximately 99% of the variability in specific heat with temperature. Consequently, accurate and reliable data

of the temperature-dependent material properties can be utilized in the iterative procedure described in Fig.3 to solve the heat transfer equation of the cooled steels on ROT.

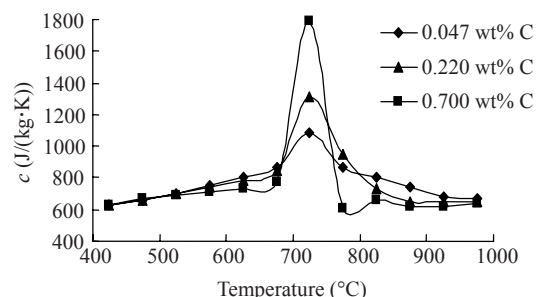


Fig.5 Steel specific heat as function of temperature

EVALUATION OF THE COUPLED MODELS

The evaluation of temperature and phase transformation models has been carried out for the prediction of different grades of steels and for different thicknesses in the 2050 mm hot strip mill of Bao Steel.

Fig.6 illustrates the calculated through-thickness temperature profile (T_C) for the head segment of a strip with a target $FT=870$ °C and a target $CT=640$ °C. The temperature is cooled down to about 720 °C through the main cooling zone then decreases slowly to about 700 °C due to air-cooling. A further temperature drop to about 640 °C is accomplished by the water sprays in the finish cooling zone. It can be seen from Fig.6 that temperature fluctuation of the strip surface is greater (than that of the quarter thickness and the central, especially when the water-cooling header strikes the strip.

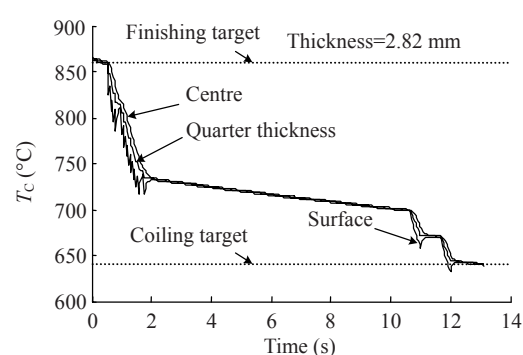


Fig.6 Temperature history along the ROT

Fig.7 shows the comparison between the measured and calculated evolution of the volume fraction X of ferrite with temperature during cooling of a carbon steel (0.220 wt% C). It can be seen that the calculated results are in good agreement with the experimental data obtained by the dilatometric analysis.

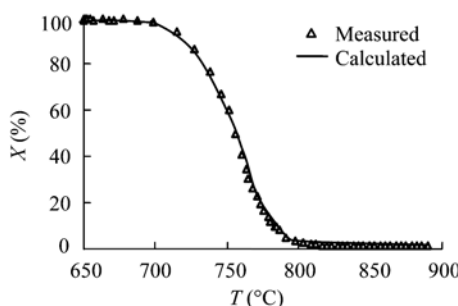


Fig.7 Comparison between measured and calculated volume fraction of ferrite during cooling

Fig.8 shows the comparison between calculated coiling temperature T_C and measured coiling temperature T_M . Over a total of 2000 coils, the calculated coiling temperature ranges from 497.5 °C to 775.4 °C, with the average error being 0.91 °C and the standard deviation 10.21 °C. Taking into consideration the phase changes during the cooling process and the knowledge of the temperature-dependent material properties, the calculated temperatures are in excellent agreement with measurements.

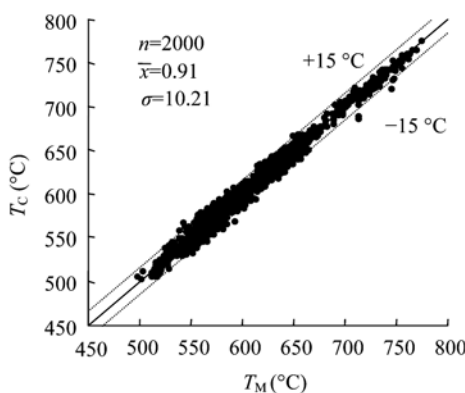


Fig.8 Comparison between measured coiling temperature and calculated coiling temperature

The versatility of the coupled models has been tested at Baosteel for strips of a thickness from 1.30 to 10.6 mm. Table 2 shows the comparison of ± 15 °C coiling temperature hit rates between the old temperature prediction system and the new system based

on the proposed temperature and phase transformation models. It can be seen that an average 11% improvement has been achieved and that the new system precisely predicts the strip temperatures in spite of the broad range of thickness of the strips.

Table 2 Comparison of ± 15 °C coiling temperature hit rates

Thickness (mm)	± 15 °C coiling temperature hit rates (%)	
	Old system	New system
1.30~2.30	82.47	95.81
2.30~4.30	81.06	94.78
4.30~6.30	86.48	95.50
6.30~8.30	88.11	96.74
8.30~10.60	84.59	95.01

CONCLUSION

(1) Coupled models based on the variation technique and the finite element method are built to evaluate the temperature history of cooled strips on the ROT. In order to access accurate predictions, the adaptive correction is adopted to calculate the heat transfer coefficients in water cooling zones and the effect of phase transformation is considered in the models.

(2) Experiments have been performed to obtain thermal material properties of three industrially used carbon steels. Based on the experimental data, models of specific heat and thermal conductivity have been established using the least squares method and utilized to solve the heat transfer equation.

(3) The comparison between the measured and the predicted results over several thousand coils of different steel grades and dimensions indicates that the new temperature setting system applied in the 2050 mm hot strip mill of Baosteel has good performance with high accuracy and versatility.

ACKNOWLEDGEMENT

The authors gratefully acknowledge Professor J.M. Zhang for his comments and Baosteel Iron & Steel Co., Ltd. for supplying the industrial data.

References

Chen, S.X., Fu, X., Zou, J., 2006. Study on finishing tem-

- perature setting system and self-adaptation of hot strip mill. *Iron and Steel*, **41**:44-48 (in Chinese).
- Han, H.N., Lee, J.K., Kim, H.J., 2002. A model for deformation, temperature and phase transformation behavior of steels on ROT in hot strip mill. *Journal of Materials Processing Technology*, **128**(1-3):216-225. [doi:10.1016/S0924-0136(02)00454-5]
- Moaveni, S., 2005. Finite Element Analysis. Pearson Education, Inc., New York, p.322-323 (in Chinese).
- Mukhopadhyay, A., Sikdar, S., 2005. Implementation of on-line ROT model in a hot strip mill. *Journal of Materials Processing Technology*, **169**(2):164-172. [doi:10.1016/j.jmatprotec.2005.04.039]
- Prieto, M.M., Ruiz, L.S., Menendez, J.A., 2001. Thermal performance of numerical model of hot strip mill runout table. *Ironmaking and Steelmaking*, **28**(6):474-480. [doi:10.1179/030192301678352]
- Serajzadeh, S., 2003. Prediction of temperature distribution and phase transformation on the ROT in the process of hot strip rolling. *Applied Mathematical Modelling*, **27**(11):861-875. [doi:10.1016/S0307-904X(03)00085-4]
- Serajzadeh, S., 2006. Prediction of temperature variations and kinetics of austenite phase change on the ROT. *Materials Science Engineering A*, **421**(1-2):260-267. [doi:10.1016/j.msea.2006.01.071]
- Singh, A., Singh, I.V., Prakash, R., 2006. Numerical solution of temperature dependent thermal conductivity problems using a meshless method. *Numerical Heat Transfer Part A: Applications*, **50**(2):125-145. [doi:10.1080/10407780500507111]
- Sun, C.G., Han, H.N., Lee, J.K., 2002. A finite element model for the prediction of thermal and metallurgical behavior of strip on ROT in hot rolling. *ISIJ International*, **42**(4):392-400. [doi:10.2355/isijinternational.42.392]
- Tan, X., Conway, P.P., Sarvar, F., 2005. Thermo-mechanical properties and regression models of alloys: AISI 305, CK 60, CuBe₂ and Laiton MS 63. *Journal of Materials Processing Technology*, **168**:152-163.
- Zhang, Y.T., Li, D.Z., Li, Y.Y., 2006. Modeling of austenite decomposition in plain carbon steels during hot rolling. *Journal of Materials Processing Technology*, **171**(2):175-179. [doi:10.1016/j.jmatprotec.2005.07.003]